Influence of substrate bias voltage on the microstructure of nc-SiO_x:H film*

Li Hui-Min(李慧敏), Yu Wei(于 威)†, Xu Yan-Mei(徐艳梅), Ji Yun(季 云), Jiang Zhao-Yi(蒋昭毅), Wang Xin-Zhan(王新占), Li Xiao-Wei(李晓苇)‡, and Fu Guang-Sheng(傅广生)

Hebei Key Laboratory of Optic-electronic Information Materials, College of Physics Science and Technology, Hebei University, Baoding 071002, *China*

(Received 27 July 2014; revised manuscript received 26 August 2014; published online 10 December 2014)

Amorphous silicon oxide containing nanocrystalline silicon grain (nc-SiO_x:H) films are prepared by a plasma-enhanced chemical vapor deposition technique at different negative substrate bias voltages. The influence of the bias voltage applied to the substrate on the microstructure is investigated. The analysis of x-ray diffraction spectra evidences the *in situ* growth of nanocrystalline Si. The grain size can be well controlled by varying the substrate bias voltage, and the largest size is obtained at 60 V. Fourier transform infrared spectra studies on the microstructure evolutions of the nc-SiO_x:H films suggest that the absorption peak intensities, which are related to the defect densities, can be well controlled. It can be attributed to the fact that the negative bias voltage provides a useful way to change the energies of the particles in the deposition process, which can provide sufficient driving force for the diffusion and movement for the species on the growing surface and effectively passivate the dangling bonds. Also the larger grain size and lower band gap, which will result in better photosensitivity, can also be obtained with a moderate substrate bias voltage of 60 V.

Keywords: nc-SiO_x:H, microstructure, substrate bias voltage

PACS: 81.07.Bc, 78.67.Bf , 84.37.+q **DOI:** 10.1088/1674-1056/24/2/028102

1. Introduction

For the past few years, silicon nanostructures have aroused great interest in improving the solar cells performance and exhibited great potential applications in LEDs, non-volatile storage devices, and third generation solar cells due to a quantum confinement effect.[1–4] Because of the advantages of lower absorption, lower refractive index, and tunable resistance,[5–8] amorphous silicon oxide containing nanocrystalline silicon grain (nc-SiO_x:H) films show great potential for their applications in the solar cells, and a large number of energy levels related to the absorptions of different wavelengths can be obtained by controlling the size of Si nanocrystal.[9]

Many groups have realized the *in situ* growth of nc-SiO_x:H film, instead of the high temperature annealing, to form the nanocrystalline silicon, and the control of the microstructure of nc-SiO_x:H films, such as defect densities, nanocrystalline size and uniformity, has become a hot point in the application of the nc-SiO_x:H films. In recent years, researchers suggested that the microstructures of Si-based films can be controlled by the application of substrate bias voltage. Bronneberg *et al.*[10] proposed that substrate bias voltage could improve the depletion of silane (SiH_4) and passivate the grain boundary of nanocrystalline Si, making it possible to prepare solar-grade films. Shen *et al.*[11] proposed a passivation effect mechanism with the substrate bias voltage. The accelerated H atoms and ions with moderate energies provided by the proper bias voltage can effectively passivate the dangling bonds, which is crucial to the quality of the growing film. However, for nc-SiO_x:H films, the deposition by plasma-enhanced chemical vapor deposition (PECVD) may result in plasma-induced defects, silicon hydrides, and some columnar structures, which hinder the carrier transport in the films.[12]

In the present paper, we provide a useful way to change the energies of the particles in the deposition process by applying a negative direct current bias voltage to the substrate, which can provide a sufficient driving force for the diffusion and movement of the species on the growing surface and effectively passivate the dangling bonds. The as-prepared nc-SiO_x:H films each have a larger crystalline size, lower defect density, and higher photosensitivity at 60 V.

2. Experiments

The nc-SiO_x:H films were deposited on P-type crystalline silicon (100) and quartz substrates at 250 °C by radio frequency (13.56 MHz, 70 W) PECVD with SiH_4, hydrogen (H_2), and nitrous oxide (N_2O) as the reaction gas. The silicon substrates were first immersed into the mixture of acetone and carbinol for 5 minutes, followed by the mixture of ammonia water and hydrogen peroxide, and finally dipped into the buffered hydrofluoric acid to remove the native silicon oxide from the surface of the substrate. The flow rates of SiH_4, H_2,

*Project supported by the Key Basic Research Project of Hebei Province, China (Grant No. 12963930D), the Natural Science Foundation of Hebei Province, China (Grant No. F2013201250), and the Science and Technology Research Projects of the Educational Department of Hebei Province, China (Grant No. ZH2012030).

†Corresponding author. E-mail: yuwei@hub.edu.cn

‡Corresponding author. E-mail: laser@hbu.edu.cn

© 2015 Chinese Physical Society and IOP Publishing Ltd

and N_2O were 1, 50, and 0.1 sccm, respectively. The chamber pressure was maintained at 78 Pa. The negative bias voltages applied to the substrate were set to be 0, 30, 60, 90, and 120 V, respectively. The corresponding samples were denoted as S1, S2, S3, S4, and S5.

The thickness values of the films were measured by a Dektak 150 proflometer. The x-ray diffraction (XRD) spectra were measured on a Bruker D8 x-ray diffracmeter with Cu Kα radiation (40 kV, 40 mA). Absorption spectra of the films were recorded with a Hitachi UV-4100 spectrometer in the range 240 nm–1100 nm. Moreover, the bonding configuration and amounts of hydrogen and oxygen content of the films could be characterized by Fourier transform infrared (FTIR) spectra measured by a Bruker TENSOR27 from 400 cm^{-1} to 4000 cm^{-1} with a resolution of 4 cm^{-1}. The lateral dark conductivity and photoconductivity were measured via a coplanar configuration by an Agilent B1500A Semiconductor Device Analyzer. The quartz substrates were used for the measurements of XRD, absorption spectra, and photosensitivity, while the FTIR and high resolution TEM (HRTEM) spectra were measured using silicon substrates.

3. Results and discussion

The film thickness and XRD measurements are performed at room temperature to obtain the structural details of the nc-SiO_x:H films and the results are illustrated in Fig. 1. Figure 1(a) shows the deposition rate with substrate bias voltage. It can be observed that the deposition rate decreases with increasing the bias voltage to 60 V, and then increases. As shown in Fig. 1(b), the XRD spectra suggest that all the samples each exhibit three diffraction peaks centered at $2\theta \sim 28.3°$, 47.1°, and 55.9°, which correspond to the (111), (220), and (311) planes of crystalline silicon, respectively.[13] The peak around 22° can be attributed to the diffraction of amorphous silicon.[14] The intensity of the XRD peak for the (111) plane is strongest, indicating that the nanocrystallites exhibit preferential growth along the (111) plane.

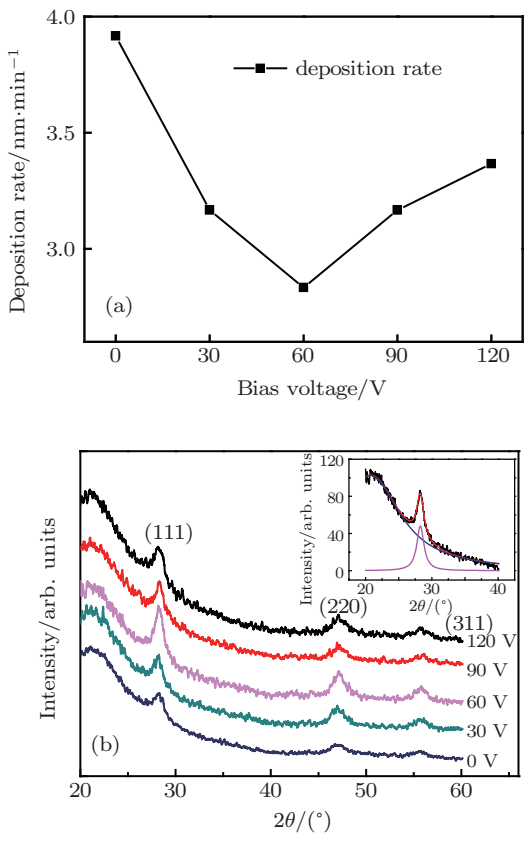


Fig. 1. (color online) (a) Variation of deposition rate with bias voltage on the substrate. (b) Experimental XRD spectra each with three diffraction peaks. The inset shows the experimental and fitted diffraction peaks of S3.

The experimental spectra can be decomposed into Gaussian peaks and the full width at half maximum (FWHM) of the fitted peak at around 28.3° can be used to calculate the average grain size of different samples by the Scherrer formula,[15] and the results are shown in Fig. 2. The grain size increases with the increase of bias voltage up to 60 V, and then decreases.

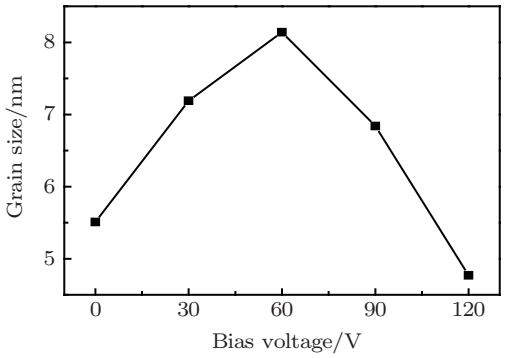


Fig. 2. Average grain size calculated by Scherrer formula versus bias voltage.

The evolutions of grain size and deposition rate can be considered as the consequence of the competition between diffusion and the etching effect. It can be observed that with the increase of the bias voltage up to 60 V, the deposition rate decreases significantly, while the size of Si nanocrystals increases to the highest point. The evolution of grain size can be explained as that the substrate bias voltage provides H atoms and ions with energy and momentum as the driving force. The accelerated H atoms with proper energy can effectively passivate the dangling bonds on the growth surface and at the interface and etch the weak Si–Si bonds,[16] benefiting the growth of nanocrystals and the reduction of the defects. These can lead to a compact and ordered microstructure, lower density of defects, and larger grain size, also a lower deposition rate. The disturbed diffusion process caused by ion bombardment also leads to the decrease of the deposition rate. After the bias voltage reaches 60 V, further increasing bias voltage would lead to the increase of the deposition rate and the decrease of the grain size. High substrate bias voltage brings about immoderate energy for H atoms and ions. The excessive etching

effect of active H leads to stopping the growth of nanocrystals. The excessive bombardment of ions causes not only the decrease in crystallization, but also the increase of the defect density in the film. Besides, the ion bombardment could transfer energy to the species and heat the growth surface, which benefits the diffusion and incubation. Moreover, the sufficient coverage of active H atoms with high bias voltage on the surface enhances the diffusion length by passivating the dangling bonds and producing local heat from H recombation reaction.[17] These aspects can effectively contribute to the increase of the deposition rate, though there exists the excessive etching effect.

Figure 3(a) shows a typical HRTEM image of S3 where it can be clearly observed that approximately 8-nm-size silicon nanocrystals are embedded in an amorphous matrix. The inset provides the SAED pattern showing three diffusion rings, which represent the (111), (220), and (311) planes of silicon. Figure 3(b) shows the EDS result of S3, and its oxygen content is nearly kept at 16 at.%.

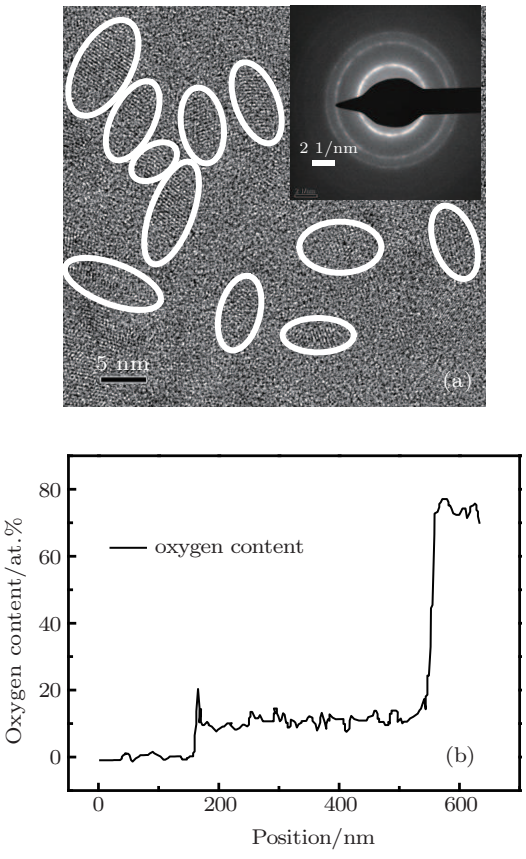


Fig. 3. Structural properties of S3 measured with HRTEM and energy-dispersive spectrometry (EDS). (a) HRTEM image with selected area electron diffraction (SAED) pattern shown in the inset. (b) Oxygen content obtained from the EDS analysis.

Figure 4 shows the FTIR spectra of the nc-SiO_x:H films. The Si–O absorption regions are located in the range 450 cm^{-1}–1300 cm^{-1}, including wagging modes in the range 450 cm^{-1}–550 cm^{-1}, bending modes in the range 550 cm^{-1}–900 cm^{-1}, and asymmetric stretching modes in the range 900 cm^{-1}–1300 cm^{-1}.[18] Like the ranges of Si–O peaks, the ranges of Si–H peaks can also be divided into three regions, including wagging modes in 620 cm^{-1}–750 cm^{-1}, bending modes in 800 cm^{-1}–1000 cm^{-1}, and stretching modes in 1900 cm^{-1}–2300 cm^{-1}.[19,20]

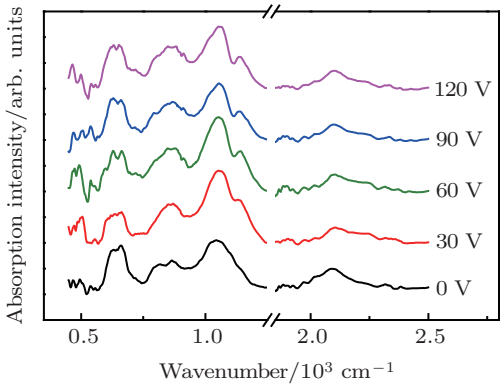


Fig. 4. (color online) FTIR absorption spectra of nc-SiO_x:H films versus bias voltage.

To gain more information about the microstructure and content of hydrogen and oxygen, the FTIR spectra are fitted by Gaussian peaks. The hydrogen content is calculated with the hydrogen absorption peak centered at 630 cm^{-1},[21,22] while the oxygen content is derived from the oxygen absorption peaks centered in the range 900 cm^{-1}–1300 cm^{-1}. The bonded-hydrogen content C_H can be calculated by numerical integration from the Si–H wagging mode by using the formula $C_H = 1/N_{Si} \times A_H \times \int(\alpha(\omega)/\omega)\mathrm{d}\omega$, where $\alpha(\omega)$ is the absorption coefficient, ω is the wavenumber, $N_{Si} = 5 \times 10^{22}$ cm^{-3} is the atomic density of the c-Si (crystalline silicon), and $A_H = 1.6 \times 10^{19}$ cm^{-2} is the proportionality constant.[23] Meanwhile, the bonded-oxygen content C_O can be similarly calculated by numerical integration from the Si–O stretching mode in 900 cm^{-1}–1300 cm^{-1} with $A_O = 9.5 \times 10^{18}$ cm^{-2}.[24] The calculated results of C_H and C_O for different nc-SiO_x:H films are plotted in Fig. 5.

Figure 5 shows the variations of C_H content and C_O content with bias voltage, and inverse correlation between C_H content and C_O content can be observed. With the increase of the bias voltage up to 60 V, the H atoms and ions gain higher energies, which is beneficial for the diffusing of the growing species and the etching of the dangling bonds along the grain boundary. As the grain size increases, the interface extends, thereby accelerating the phase separation. The increased bias voltage also increases the density of the oxygen particles that reach the growth surface, accompanied by the enhanced possibility of a desorption reaction caused by the oxygen incursion and the increase of the oxygen content. It can be seen that from S3 the fitted result is in good agreement with the result extracted from the EDS, which is shown in Fig. 3(b). With the further increase of bias voltage, the sufficient coverage of active H atoms on the surface contributes to preventing the oxygen incursion. The excessive etching of the weak Si–Si bonds

and dangling bonds would result in a higher hydrogen content and smaller grain size. In the plasma, the active H reacts with oxygenated particles, resulting in less oxygen content on the growth surface and a lower probability of desorption. This leads to the decrease of oxygen content.

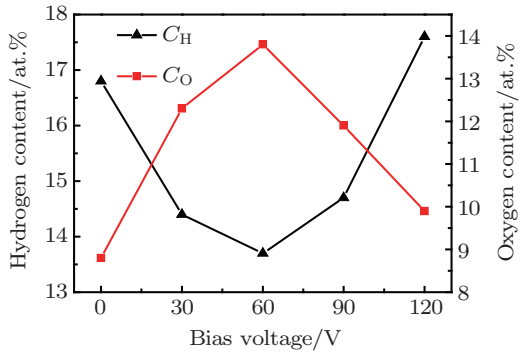


Fig. 5. (color online) Hydrogen content (C_H) and oxygen content (C_O) of nc-SiO_x:H films versus bias voltage.

The evolutions of the absorption peak intensities of FTIR spectra indicate the variations of the microstructure of nc-SiO_x:H films. In order to obtain the detailed bond structures of nc-SiO_x:H films, the Si–H bond region and the Si–O bond region are fitted by certain Gaussian peaks. Figure 6(a) presents the detailed structures of the Si–O stretching mode peaks in 900 cm^{-1}–1300 cm^{-1}, in which six different bonding configurations of oxide can be identified. The peaks centered at 980, 1012, 1034, and 1076 cm^{-1} are related to the stretching vibration modes of $HSi(Si_2O)$, $HSi(SiO_2)$, $HSi(O_3)$, and $Si(O_4)$, respectively. The absorption peak centered at 1150 cm^{-1} is related to the vibration of the oxygen in the $Si(O_4)$ network.[18,20] The peak at 1100 cm^{-1} is attributed to the crystal substrate surface oxidation absorption.[25,26] The four peaks are divided into two groups, and the peaks centered at 980 cm^{-1} and 1012 cm^{-1} correspond to the Si-rich Si–O vibrations, while the others correspond to the O-rich Si–O vibrations. The intensities of the $I_{Si-rich}$ ($I_{Si-rich} = (I_{980+1012})/(I_{980+1012+1034+1076})$) and I_{O-rich} ($I_{O-rich} = (I_{1034+1076})/(I_{980+1012+1034+1076})$) are shown in Fig. 6(b). With the increase of bias voltage, the oxidation reaction is enhanced gradually and the interface increases due to the larger grain size, which would contribute to the increased oxygen incursion. The incorpation of oxygen may release some strains and fill some defects. However, the further increase of the bias voltage would induce an excessive etching effect, which would prevent the oxygen from entering into the films. All these give the evolution of $I_{Si-rich}$ and I_{O-rich} as shown in Fig. 6(b).

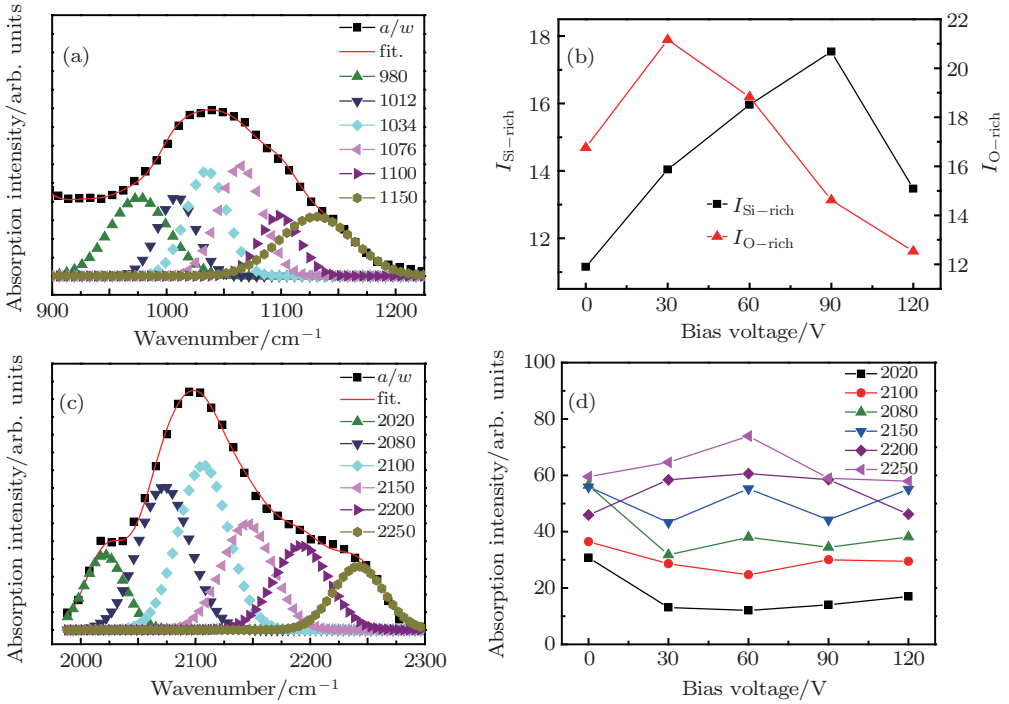


Fig. 6. (color online) (a) FTIR absorption spectrum for Si–O stretching mode of S3. The square dotted line is the experimental curve, while the solid line is the fitted line across the whole zone and the others are the Gaussian type peaks centered at different wavenumbers. (b) Plots of $I_{Si-rich}$ and I_{O-rich} in the nc-SiO_x:H films versus bias voltage. (c) Like Fig. 6(a), an FTIR absorption spectrum for the Si–H stretching mode of S3 and its fitted peaks. (d) Absorption intensities of peaks centered in the range 1900 cm^{-1}–2300 cm^{-1}.

Based on the above investigation, a clear physical process of the microstructure affected by the substrate bias voltage can be seen. When the low substrate bias voltage is applied, the possibilities of $HSi(Si_2O)$ and $HSi(SiO_2)$ bond configurations are reduced, while $HSi(O_3)$ and $Si(O_4)$ are activated, resulting in Si/SiO_x phase separation. Furthermore, a higher voltage (more than 60 V) would improve the nucleation on the growth surface and enhance the reaction between the active H

and surface O, leading to the decrease of $HSi(O_3)$ and $Si(O_4)$ bond configuration. While the incorporation of the active H in both Si-rich zone and O-rich zone will present as the relative increase of $HSi(Si_2O)$ and $HSi(SiO_2)$ bond configuration possibilities with a bias voltage more than 60 V. The results mentioned above also indicate the oxygen content evolutions in the nc-SiO_x:H films.

Figure 6(c) shows the Gaussian fitting results of Si–H stretching mode peaks in the range 1900 cm^{-1}–2300 cm^{-1}, and six peaks are obtained relevant to the detailed structures of the nc-SiO_x:H films. The vibration peaks at 2020 cm^{-1} and 2100 cm^{-1} are related to the SiH and SiH_2 absorption in the amorphous silicon zone[27] corresponding to the H bonded to multivacancies as well as to a nano-sized void surface.[28] As shown in Fig. 6(d), the peak intensities of 2020 cm^{-1} and 2100 cm^{-1} show an upward parabola form with bias voltage increasing. With the application of substrate bias voltage, the densities of vacancies and voids could be well controlled with the best performance obtained at 60 V. The peaks at 2080, 2150, 2200, and 2250 cm^{-1} are related to $SiH(SiH(Si_2O))$, $SiH_2(SiH_2(SiO))$, $SiH(SiO_2)(SiH_2(O_2))$, and $SiH(O_3)$ absorption in the SiO_x zone.[16] The I_{2200} and I_{2250} related to the O-rich bonding each reach the corresponding highest point at 60 V, which is in agreement with the evolution of the oxygen content. All the absorption intensity variations of the Si–H stretching mode peaks are shown in Fig. 6(d), which indicate that high-quality nc-SiO_x:H films with lower defect density and better quality can be achieved through the control of the substrate bias voltage, and the best deposition parameter is 60 V.

Figure 7(a) shows the absorption spectra of samples deposited at different bias voltages, and the band gap and B factor can be calculated by the Tauc formula $(\alpha h\nu)^{1/2} = B(h\nu - E_g)$,[29] where α is the absorption coefficient, $h\nu$ is the energy of the incident light, B indicates the disorder degree, and E_g is the optical band gap. From the calculated results shown in Figs. 7(b) and 7(c), it can be obtained that with the increase of bias voltage, E_g and the B factor first decrease, and then increase. This may be caused by the larger grain size followed by the smaller band gap and more ordered microstructure with higher voltage when it is below 60 V. When the voltage is enhanced further, the excessive etching stops the continous growth of the grain and the immoderate bombardment damages the films that have deposited on the substrate. These lead to the decrease of grain size and the increase of defect density, accompanied by a larger band gap and disorder degree.

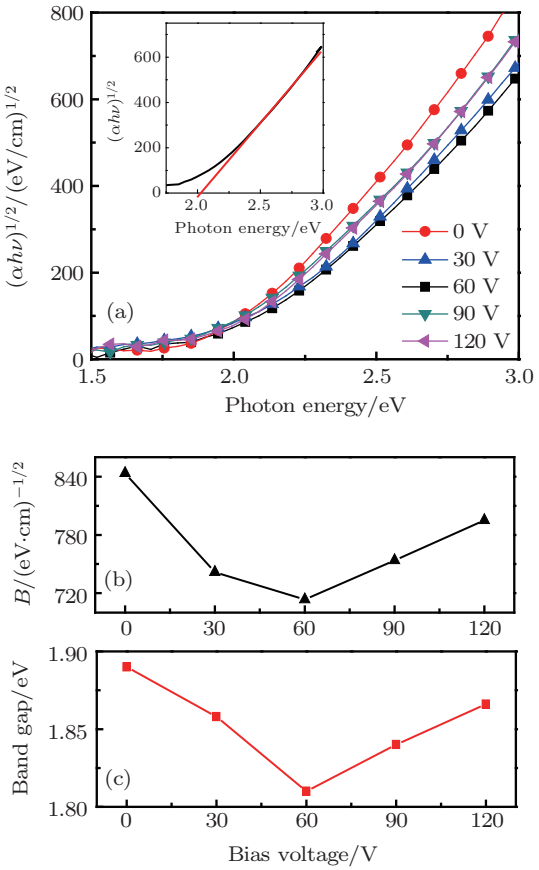


Fig. 7. (color online) (a) Relations between $(\alpha h\nu)^{1/2}$ and the photon energy, and the inset shows the fitting which gives the band gap. (b) and (c) Variations of B factor and band gap with bias voltage.

Figure 8 shows the photosensitivity of the nc-SiO_x:H film with bias voltage. The x is the stoichiometric ratio of O/Si and corresponding to the increasing bias voltage, the values of x are 0.12, 0.17, 0.19, 0.16, and 0.14, respectively. With the increase of bias voltage, the photosensitivity first increases, and then decreases. The biggest photosensitivity is about 1500, and it is obtained at 60 V. Good photosensitivity means a high carrier generation rate, and it usually corresponds to low E_g. Better ordered microstructure, low defect density, and high photosensitivity of S3 suggest that good-quality nc-SiO_x:H films can be obtained which are very useful in the application of solar cells.

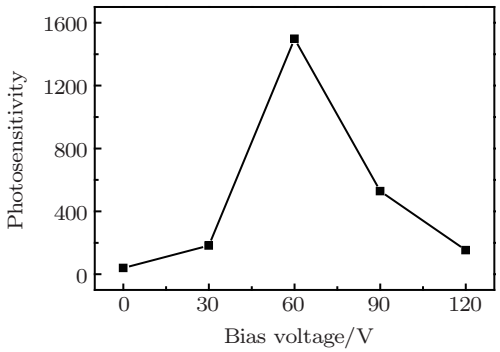


Fig. 8. Photosensitivity of the nc-SiO_x:H film versus bias voltage.

4. Conclusions

In this paper, we perform an overall study of the influences of substrate bias voltage on the microstructures of nc-SiO_x:H films deposited by the PECVD technique. XRD and absorption spectra are used to elucidate the structure evolution and film growth with substrate bias voltage. By varying the bias voltage, larger silicon grain size, better ordered microstructure, and lower defect density are achieved. The moderate voltage provides the H atoms and ions with appropriate energies resulting in a longer diffusion length and better etching of the dangling bonds, which contribute to the good-quality of films. Furthermore, good photosensitivity can be obtained at 60 V, which means that a higher carrier generation rate is achieved. The present work offers a valuable means to control the growth of nc-SiO_x:H film by adjusting the substrate bias voltage.

References

[1] Mirabella S, Agosta R, Franzò G, Crupi I, Miritello M, Savio R L, Stefano M A D, Di Marco S, Simone F and Terrasi A 2009 *J. Appl. Phys.* **106** 103505

[2] Ma J, Ni J, Zhang J J, Liu Q, Hou G F, Chen X L, Zhang X D and Zhao Y 2014 *Sol. Energy Mater. Sol. Cells* **123** 228

[3] Zhang X D, Zheng X X, Xu S Z, Lin Q, Wei C C, Sun J, Geng X H and Zhao Y 2011 *Chin. Phys. B* **20** 108801

[4] Guo Y Q, Huang R, Song J, Wang X, Song C and Zhang Y X 2012 *Chin. Phys. B* **21** 066106

[5] Cuony P, Marending M, Alexander D T L, Boccard M, Bugnon G, Despeisse M and Ballif C 2010 *Appl. Phys. Lett.* **97** 213502

[6] Cuony P, Alexander D T L, Löfgren L, Krumrey M, Marending M, Despeisse M and Ballif C 2011 *MRS Proceedings* **1321** mrss11-1321-a12-02

[7] Yan B J, Yue G Z, Sivec L, Yang J, Guha S and Jiang C S 2011 *Appl. Phys. Lett.* **99** 113512

[8] Veneri P D, Mercaldo L V and Usatii I 2010 *Appl. Phys. Lett.* **97** 023512

[9] Xia Z Y, Han P G, Xu J, Chen D Y, Wei D Y, Ma Z Y, Chen K J, Xu L and Huang X F 2007 *Chin. Phys. Lett.* **24** 2657

[10] Bronneberg A C, Cankoy N, van de Sanden M C M and Creatore M 2012 *J. Vac. Sci. Technol. A* **30** 061512

[11] Wen C, Xu H, Liu H, Li Z P and Shen W Z 2013 *Nanotechnology* **24** 455602

[12] Yu W, Wang J T, Li Y, Guo S G, Zhu H R and Fu G S 2013 *J. Synth. Cryst.* **42** 1035 (in Chinese)

[13] Comedi D, Zalloum O H Y, Irving E A, Wojcik J, Roschuk T, Flynn M J and Mascher P 2006 *J. Appl. Phys.* **99** 023518

[14] Wu X, Ossadnik C, Eggs C, Veprek S and Phillipp F 2002 *J. Vac. Sci. Technol. B* **20** 1368

[15] Langford J I and Wilson A J C 1978 *J. Appl. Crystallogr.* **11** 102

[16] Matsuda A 1999 *Thin Solid Films* **337** 1

[17] Veprek S, Iqbal Z and Sarott F A 1982 *Phil. Mag. B* **45** 137

[18] He L, Inokuma T, Kurata Y and Hasegawa S 1995 *J. Non-Cryst. Solids* **185** 249

[19] Lucovsky G, Nemanich R J and Knights J C 1979 *Phys. Rev. B* **19** 2064

[20] Tsu D V, Lucovsky G and Davidson B N 1989 *Phys. Rev. B* **40** 1795

[21] Brodsky M H, Cardona M and Cuomo J J 1977 *Phys. Rev. B* **16** 3556

[22] Kroll U, Meier J, Shah A, Mikhailov S and Weber J 1996 *J. Appl. Phys.* **80** 4971

[23] Fang C J, Gruntz K J, Ley L, Cardona M, Demond F J, Müller G and Kalbitzer S 1980 *J. Non-Cryst Solids* **35** 255

[24] Lucovsky G, Yang J, Chao S S, Tyler J E and Czubatyj W 1983 *Phys. Rev. B* **28** 3225

[25] Atkins T M, Cassidy M C, Lee M Y, Ganguly S, Marcus C M and Kauzlarich S M 2013 *ACS Nano* **7** 1609

[26] Vaccaro, Sciortino L, Messina F, Buscarino G, Agnello S and Cannas M 2014 *Appl. Surf. Sci.* **302** 62

[27] Han D X, Wang K D, Owens J M, Gedvilas L, Nelson B, Habuchi H and Tanaka M 2003 *J. Appl. Phys.* **93** 3776

[28] Smets A H M, Kessels W M M and van de Sanden M C M 2003 *Appl. Phys. Lett.* **82** 1547

[29] Li T, Kanicki J, Kong W and Terry F L Jr 2000 *J. Appl. Phys.* **88** 5764